Data - Model Synchronization in Extended Kalman Filters for Accurate Online Traffic State Estimation

Thomas Schreiter (corresponding author)
TRAIL Research School
Delft University of Technology, Stevinweg 1, 2628 CN Delft, The Netherlands
t.schreiter@tudelft.nl, phone: +31 15 27 81723

Chris van Hinsbergen
TRAIL Research School
Delft University of Technology, Stevinweg 1, 2628 CN Delft, The Netherlands
c.p.i.j.vanhinsbergen@tudelft.nl, phone: +31 15 27 86044

Frank Zuurbier
TRAIL Research School
Delft University of Technology, Stevinweg 1, 2628 CN Delft, The Netherlands
f.s.zuurbier@tudelft.nl, phone: +31 15 27 83346

Hans van Lint
Delft University of Technology, Stevinweg 1, 2628 CN Delft, The Netherlands
j.w.c.vanlint@tudelft.nl, phone: +31 15 27 85061

Serge Hoogendoorn
Delft University of Technology, Stevinweg 1, 2628 CN Delft, The Netherlands,
s.p.hoogendoorn@tudelft.nl, phone: +31 15 27 85475

June 27, 2010

Abstract

Real-time freeway traffic state estimation plays an important role in Dynamic Traffic Management (DTM) and Advanced Traveler Information Systems (ATIS). One of the model-driven estimation techniques used in practice is based on the Extended Kalman Filter (EKF). It consists of two components: the Predictor forecasts the traffic state over a short period of time, usually a few seconds; the Corrector fuses the traffic state with online data, observed by induction loops, which are usually aggregated over one minute. Currently, in many approaches, the traffic state is corrected only once, namely as soon as the observation becomes available.

In this paper it is shown that this correction time scheme does not fully make use of all the available data. A correction time scheme is proposed, which synchronizes the Correction step of the EKF with the aggregation period of the data. Experiments with both synthetic and real data show improvements in the estimation quality.

1 INTRODUCTION

Freeway traffic state estimation plays a fundamental role in controlling the traffic via Dynamic Traffic Management (DTM) and Advanced Traveler Information Systems (ATIS). Often, DTM and ATIS systems require the state estimates to be available in real-time.

For this purpose, sensors like dual-loop detectors provide data about traffic variables such as flow and speed. These are used in traffic state estimators to fuse the data to an accurate image of the current traffic state, usually represented by a density vector. The observations are usually incomplete, noisy and local, so that interpolation between them is necessary.

There are two categories of parameterized traffic state estimators. Firstly, there are data-driven methods that only use observations to obtain the current state. An example is the "Adaptive Smoothing Method" [1] and its various extensions [2, 3] and calibrators [4].

Secondly, there are model-driven methods that use both observations and a traffic model with predictive features to estimate the current state: the recursive Bayesian filters with the widely used Kalman Filter approaches. Such a filter is divided into two components; the Prediction step forecasts the traffic state over a short time; and the Correction step fuses real-time observations with the current traffic state prediction. Examples of Kalman Filter approaches are Renaissance [5], Fastlane combined with an Extended Kalman Filter [6], a multi-class realtime traffic surveillance model based on the Unscented Kalman Filter [7], a filter approach based on the Markov Compartment Model [8], a SCAAT Kalman Filter [9] and an Ensemble Kalman Filter [10].

Define x_k to be the traffic state, for example a vector of densities. Define h to be the observation function that maps the traffic state to a traffic measurement, for example a fundamental diagram that maps density to flow. In Kalman Filter modeling, the observations $y_k = h(x_k)$ are based on one single time step k only. This means that the size of the time step should be equal to the measurement interval. However, in the traffic state estimators cited above, this condition is not met: loop detectors aggregate the speed and flow over a period of $\Delta t_{\text{obs}} = 1\,\text{min}$, whereas the system state represents the traffic over a significantly shorter period, for example $\Delta t_{\text{pred}} = 3\,\text{s}$. An observation therefore contains information not just over one time step, but over $\eta := \frac{\Delta t_{\text{obs}}}{\Delta t_{\text{pred}}}$ multiple time steps, namely from the current time step k to time step $l := k - \eta + 1$. Due to the structure of Kalman Filters, only the current system state x_k is corrected, whereas the previous states $x_{l,\dots,k-1}$ remain unchanged. The data observed are therefore not synchronized with the Kalman Filter model.

In this paper, a method to overcome this error by a different correction timing scheme is presented. In this scheme, at all time steps that are observed by sensors, the Correction of the EKF is applied. Since loop detectors observe the traffic state continuously, the Correction step is applied at every time step (Section 3). This proposed correction timing scheme is tested with both synthetic data and real data (Section 4). The results show an improvement of the filter quality (Section 5) compared with the current approaches in practice.

2 THE EXTENDED KALMAN FILTER AND THE LWR MODEL

In this section, first the macroscopic LWR model is described. Second, the structure of the Extended Kalman Filter is defined.

2.1 The LWR Model

The traffic is described by macroscopic variables, such as density r, flow q and speed v. The traffic model used in this paper is the LWR model [11, 12]. It is founded on the conservation law of

vehicles

$$\frac{\partial r}{\partial t} + \frac{\partial q}{\partial x} = 0 \ . \tag{1}$$

In order to solve (1) numerically, the highway network is spatially discretized into cells i of length Δx_i and temporally discretized into time steps of length Δt_{pred}. Each cell i is characterized by an equilibrium flow-density relation Q_i^{fd}, often referred to as fundamental diagram.

The density $r_{i,k}$ of a cell i at time step k evolves to the next time step by the discretized conservation law of vehicles:

$$r_{i,k+1} = r_{i,k} + \frac{\Delta t_{\text{pred}}}{\Delta x_i} \cdot \left(q_{i,k}^{\text{in}} - q_{i,k}^{\text{out}}\right) \ . \tag{2}$$

Here, an explicit time stepping is used; nevertheless, also different schemes are applicable. For a discussion on this topic, see [13]. The inflow $q_{i,k}^{\text{in}}$ is the flow of vehicles entering cell i at time step k; similarly the outflow $q_{i,k}^{\text{out}}$ is the flow of vehicles leaving cell i at time step k. Within a road stretch with no merges or bifurcations,

$$q_{i,k}^{\text{out}} = q_{i+1,k}^{\text{in}} \tag{3}$$

holds. In this contribution, these fluxes between cells are determined by the Godonov minimal-supply-and-demand scheme [14]

$$q_{i,k}^{\text{out}} = \min(D_{i,k}, S_{i+1,k}) \ , \tag{4}$$

with traffic flow demand $D_{i,k}$ of cell i at time step k and traffic flow supply $S_{i+1,k}$ of cell $i+1$ at time step k. Those, in turn, depend on the current densities and the fundamental diagram of those cells:

$$D_{i,k} = \begin{cases} Q_i^{\text{fd}}(r_{i,k}) & \text{if } \mathit{ff}_{i,k} \\ q_i^{\text{cap}} & \text{if } cong_{i,k} \end{cases} \ , \tag{5}$$

$$S_{i,k} = \begin{cases} q_i^{\text{cap}} & \text{if } \mathit{ff}_{i,k} \\ Q_i^{\text{fd}}(r_{i,k}) & \text{if } cong_{i,k} \end{cases} \ , \tag{6}$$

where $\mathit{ff}_{i,k}$ and $cong_{i,k}$ indicate free-flow and congested traffic of cell i at time k, respectively, and q_i^{cap} is the capacity of cell i.

2.2 The Extended Kalman Filter (EKF)

This section describes the structure of the Extended Kalman Filter (EKF) [15]. In addition, the EKF is applied to the LWR model and the loop detector model.

The traffic system state

$$\tilde{x}_k = \begin{bmatrix} r_{1,k} & r_{2,k} & \dots & r_{I,k} \end{bmatrix}^{\text{T}} \tag{7}$$

is modeled over discrete time steps k as the densities $r_{i,k}$ of the cells i. In the following, the two components of the EKF, Prediction step and Correction step, are explained.

Prediction Step

In the Prediction step of the EKF, the LWR model (2) is used as system function f to model the evolution of the system state and the error covariance over time:

$$x_{k+1}^{\mathrm{p}} = f(x_k^{\mathrm{e}}) \tag{8}$$

$$C_{k+1}^{\mathrm{p}} = F_k C_k^{\mathrm{e}} F_k^{\mathrm{T}} + Q_k \ , \tag{9}$$

with x_{k+1}^{p} as the predicted mean system state at time $k+1$, x_k^{e} as the estimated mean system state at time k, C_{k+1}^{p} the predicted covariance at time $k+1$, C_k^{e} the estimated covariance at time k, Q_k at the system noise matrix, and F_k as the linearization of f at the current time step:

$$F_k = \left.\frac{\partial f}{\partial x}\right|_{x=x_k^{\mathrm{e}}} \ . \tag{10}$$

Correction Step

In the Correction step of the EKF, the observation function h models the relation between the system state and the sensor output. Here, dual-loop detectors are used as sensors. Such a detector is modeled by the fundamental diagram: every dual-loop detector m is placed within a cell i, observing time-mean speed $y_{m,k}^{\mathrm{v}}$ and flow $y_{m,k}^{\mathrm{q}}$. Every observed cell is therefore related to the observation by its fundamental diagram:

$$y_{m,k} = \begin{bmatrix} y_{m,k}^{\mathrm{q}} \\ y_{m,k}^{\mathrm{v}} \end{bmatrix} = \begin{bmatrix} Q_i^{\mathrm{fd}}(r_{i,k}) \\ V_i^{\mathrm{fd}}(r_{i,k}) \end{bmatrix} \ , \tag{11}$$

where the speed-density fundamental diagram $V_i^{\mathrm{fd}}(r_{i,k})$ is derived by the the flow-density fundamental diagram $Q_i^{\mathrm{fd}}(r_{i,k})$ via the transportation equation:

$$V_i^{\mathrm{fd}}(r_{i,k}) = \frac{Q_i^{\mathrm{fd}}(r_{i,k})}{r_{i,k}} \ . \tag{12}$$

The mean system state and the covariance matrix are updated by the Kalman Filter equations [16]:

$$x_k^{\mathrm{e}} = x_k^{\mathrm{p}} + K_k \left(y_k - h(x_k^{\mathrm{p}})\right) \tag{13}$$

$$C_k^{\mathrm{e}} = C_k^{\mathrm{p}} - K_k H_k C_k^{\mathrm{p}} \tag{14}$$

$$K_k = \frac{C_k^{\mathrm{p}} H_k^{\mathrm{T}}}{H_k C_k^{\mathrm{p}} H_k^{\mathrm{T}} + R_k} \ , \tag{15}$$

with R_k as the observation noise matrix, and H as the linearization of h at the current time step:

$$H_k = \left.\frac{\partial h}{\partial x}\right|_{x=x_k^{\mathrm{p}}} \ . \tag{16}$$

As described in (8) - (16), the Prediction and Correction steps are recursively connected. To start the loop in the recursive filter at $k=0$, the system state x_0^{e} and the error covariance C_0^{e} are initialized.

The Prediction step in a recursive filter is applied exactly once per time step to evolve the system over time. The Correction step, on the other hand, is applied dependent on the availability of the observations. If there are multiple observations available, then multiple Correction steps are applied in one time step. In contrast, if there is no observation available, then the Correction step is not performed and the predicted state is directly fed into the next Prediction step.

3 CORRECTION TIMING SCHEMES

Two different correction timing schemes are compared in this paper, which are explained in the following.

3.1 The classic correction time scheme

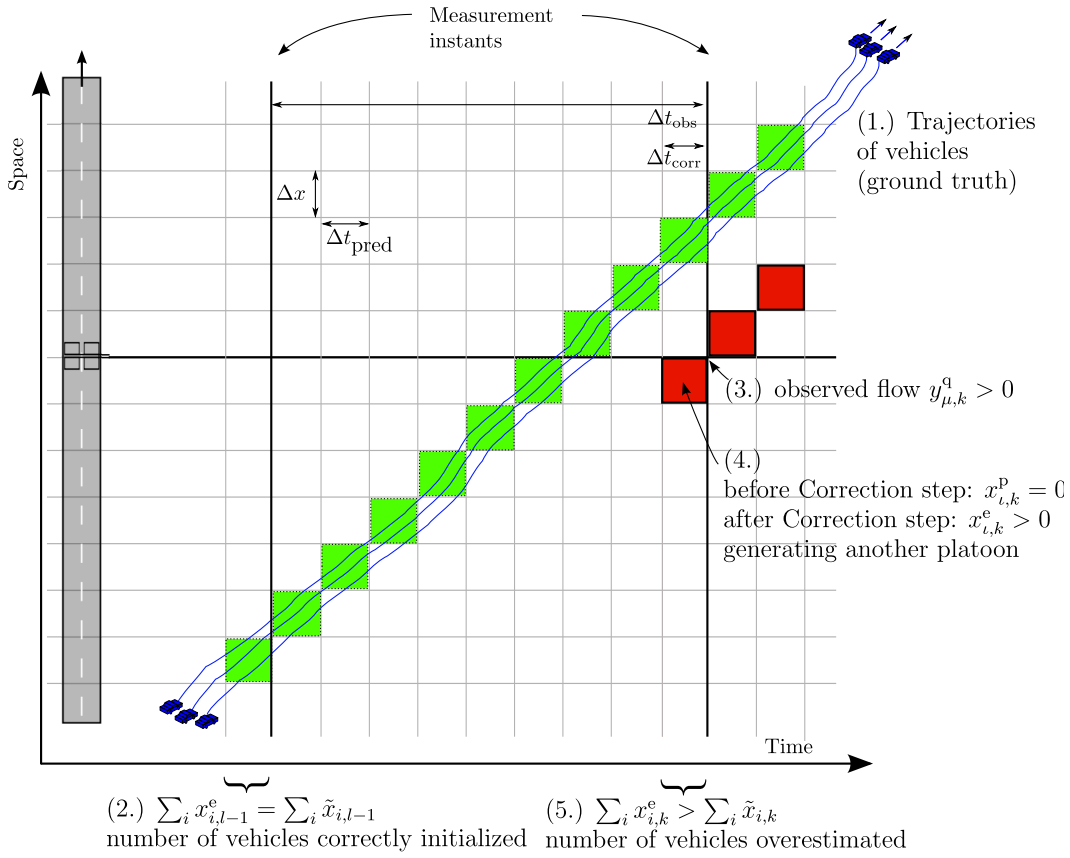

FIGURE 1 : **Principle of the *classic* correction time scheme: the Correction step of the EKF is applied once for every observation**

In the classic correction time scheme, the observation y_k is used in the Kalman Filter *once*, namely to correct the predicted system state x_k. Since the observations contain information over more than one time step, this method induces an error in the corrected system state as the following example explains.

Example 1: To illustrate how this error is induced, consider a road stretch as shown in Figure 1. A platoon of vehicles is traveling at free-flow speed (1.). The filter is initialized with the true state (2.). The first cell is in free-flow conditions, the other cells have zero density. The total density in the filter state matches the true number of vehicles.

Dual-loop detectors are installed observing the flow aggregated over period Δt_{obs}. Let detector μ be installed in cell ι. As soon as the platoon passes the detector, it observes a non-zero flow (3.), $y^{\text{q}}_{\mu,k} > 0$. This observation is aggregated over Δt_{obs} and used to correct the density of the cell ι. However, at the end of the observation period the platoon has moved further downstream. Cell ι now contains zero density in the model, $x^{\text{p}}_{\iota,k}$. Since this cell has zero density but the flow

observed is greater than zero, the state is corrected to a non-zero density (4.), $x^{\mathrm{e}}_{\iota,k} > 0$. In other words, a second platoon is generated in the estimate of the Extended Kalman Filter.

The total density estimated is now higher than the ground truth density (5.). To conclude, a previously correct estimate of the state was fused with a correct observation and led to an incorrect state. The reason is that the correction period Δt_{corr} is not synchronized with the observation period Δt_{obs}.

Note that a similar error occurs when the platoon is coincidently located in the detector cell during the Correction step. Then the density is of that cell is "corrected" to a lower value, since the flow observed is lower than the flow of that cell. In this case, vehicles would be removed, also leading an erroneous estimate.

The same error also occurs in congestion, when a stop-and-go wave is traveling over multiple cells during one observation period. Here, too, the state of only one cell is corrected, thereby inducing an error.

3.2 The fully-recursive correction time scheme

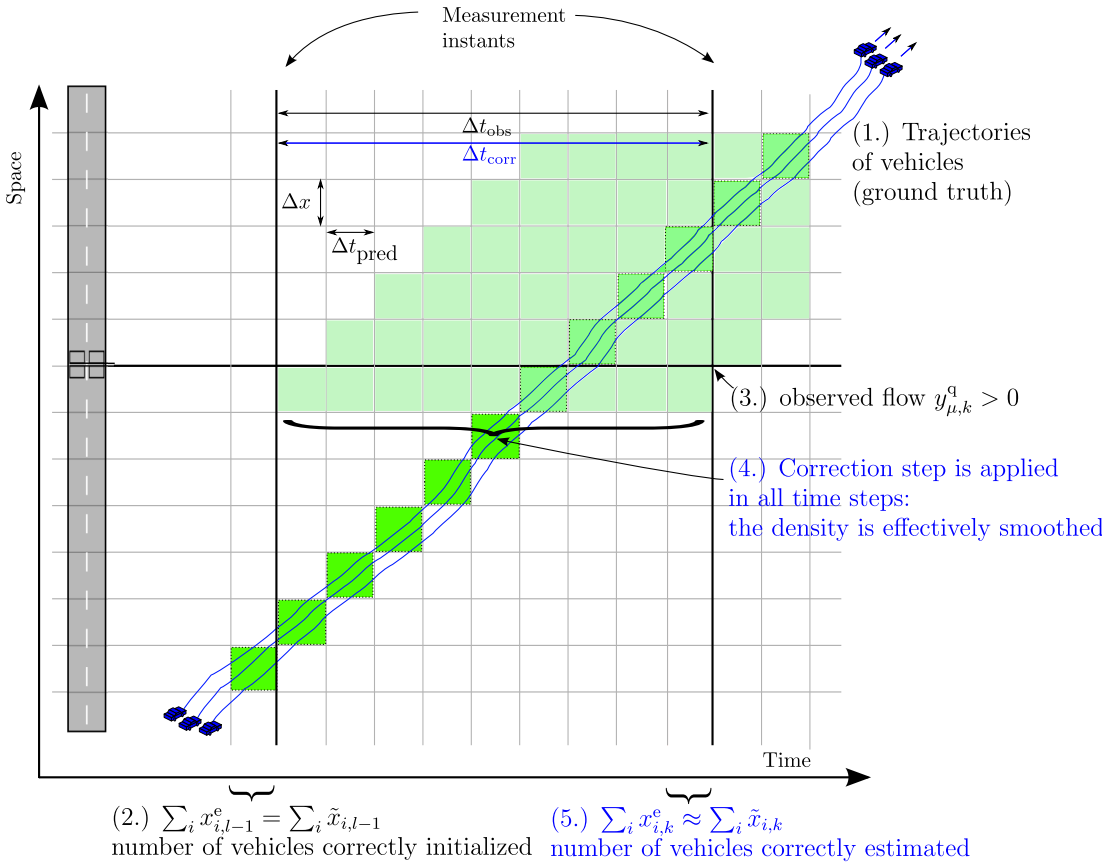

FIGURE 2 : Principle of the *fully-recursive* correction time scheme: the Correction step of the EKF is applied in every time step

To overcome the issue presented in the previous section, a fully-recursive correction time scheme is proposed that avoids the errors described above. The observation y_k is aggregated over

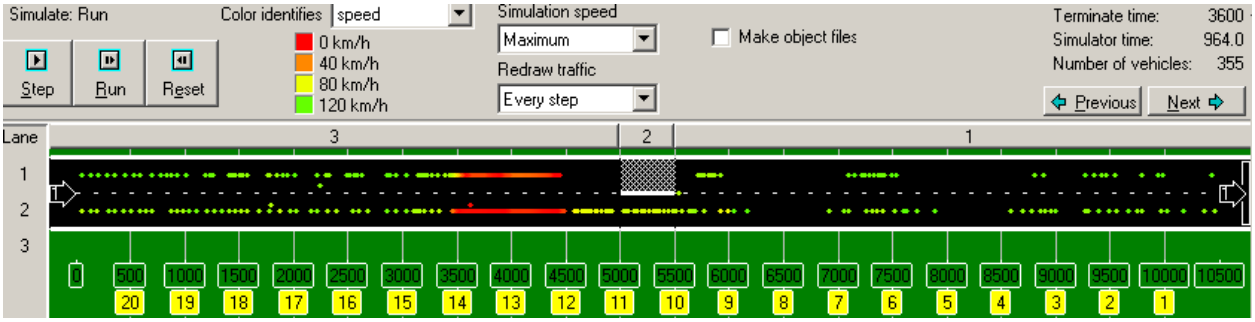

FIGURE 3 : **Screenshot of microscopic simulator Fosim with the following simulation scenario: a two-lane highway stretch with a one-lane bottleneck, causing congestion (red dots). Dual-loop detectors (yellow boxes) observe the highway every 500 m and every 60 s.**

period Δt_{obs} and is therefore influenced by multiple states $x_{l,\dots,k}$. In the fully-recursive correction time scheme, all these states are corrected by applying the Correction step of the EKF in *every* time step. An observation y_k is therefore fused sequentially with all contributing states $x_{l,\dots,k}$. This procedure leads to a scheme in the EKF, where the Prediction and the Correction step are applied alternately.

Example 2: The principle of the fully-recursive correction time scheme is illustrated in Figure 2. The setup is similar to the one of the classic scheme: a platoon of vehicles travels along the road (1.), the filter is correctly initialized (2.) and the detector observes a non-zero flow (3.). In the fully-recursive correction time scheme, however, the correction period is synchronized with the observation period.

The observation is therefore used in every time step to correct the state of the detector cell (4.). In the cases where the detector cell is empty, the state is corrected to a slightly higher density. In contrast, in the one case where the detector cell contains a non-zero density, the state is strongly corrected towards a lower density. Essentially, the platoon is smoothed out over the observation period, whereas the total density is preserved (5.). To conclude, a previously correctly estimate of the state was fused with a correct observation and preserved the total number of vehicles.

4 EXPERIMENTAL SETUP

The correction timing schemes are compared in two experiments. In the first experiment (Section 4.1), a highway of ten kilometer length including a bottleneck is simulated, using the validated microscopic traffic simulator Fosim [17]. In the second experiment (Section 4.2), real data from NGSIM [18] are used.

The raw data sets of both experiments provide complete trajectory data of vehicles. These are used to calculate the ground truth density by Edie's definition [19]. The loop detector data of flow and speed were calculated by aggregating vehicle passages over virtual detectors.

The remainder of this section explains the road network and the setup of the EKF parameters of both experiments. Finally, Section 4.3 defines the performance measurements used for evaluating the filter quality of the correction timing schemes.

4.1 Experimental setup based on synthetic data

The scenario is a two-lane highway stretch with a bottleneck where one lane is closed. A screenshot of this scenario in Fosim is shown in Figure 3. The total length of the road stretch is 10.5 km. The lane drop has a length of half a kilometer, but since the vehicles merge earlier, the effective bottleneck length is one kilometer. The detectors (yellow boxes) are placed 500 m apart, providing time-mean speed and flow observations aggregated over 60 s.

The simulation time is one hour. At the beginning of the simulation, the traffic demand is undersaturated, then increasing to oversaturated and maintaining this value for half an hour, so that a jam emerges (red dots in Figure 3). Near the end of the simulation, the demand is undersaturated again, so that the jam dissolves completely.

The EKF is based on a discretized LWR model (2) with cell length $\Delta x = 100\,\mathrm{m}$ and time step length $\Delta t_{\text{pred}} = 3\,\mathrm{s}$, which leads to $I = 105$ cells and $K = 1200$ time steps. This discretization complies with the Courant-Friedrichs-Levy condition [20] and a free speed of $v^{\text{free}} = 120\,\mathrm{km/h}$. The fundamental diagrams of the 2-lane and the 1-lane section were estimated in FOSIM; these are shown in Figure 4. The specific values are: a critical speed of 100 km/h; a jam density of 256 veh/km and 128 veh/km, respectively; and a capacity of 4500 veh/h and 2400 veh/h, respectively. The inflow into the filter model is set to a fixed value of $1000\,\mathrm{veh/h}$.

The system noise matrix Q was estimated in FOSIM as well. Both the traffic prediction model f and FOSIM were initialized with the same true state $\tilde{x}_k$. Then, a prediction step was performed (8) and Fosim was run for a time step $\Delta t_{\text{pred}} = 3\,\mathrm{s}$, resulting in a predicted mean state $x^{\text{p}}_{k+1} = f(\tilde{x}_k)$ and a true state $\tilde{x}_{k+1}$, respectively. This procedure was repeated many times. Finally, the system noise matrix

$$Q = Cov\left\{\tilde{x}_{k+1} - f(\tilde{x}_k)\right\} \tag{17}$$

is set to the covariance matrix of the errors between them. This calibration procedure showed that the diagonal elements of Q are approximately $5\,\mathrm{veh^2/km^2}$ in free-flow conditions and $10\,\mathrm{veh^2/km^2}$ in congested conditions. Therefore, Q_k was set to a diagonal matrix with values of 5 in case of free-flow, and 10 in case of congestion.

The observation noise matrix R was obtained in a similar procedure. The variance for flow observations was calibrated to $50000\,\mathrm{veh^2/h^2}$ and for speed observations to $100\,\mathrm{km^2/h^2}$. The system state is initialized with an empty road and a variance of $10\,\mathrm{veh^2/km^2}$ of each cell.

In the classic time stepping approach, the Correction step is applied every $\Delta t_{\text{corr}} = \Delta t_{\text{obs}} = 60\,\mathrm{s}$. In the fully-recursive approach, the Correction step is applied in every time step; therefore $\Delta t_{\text{corr}} = \Delta t_{\text{pred}} = 3\,\mathrm{s}$.

Ten Monte Carlo simulations were performed, where the driving behavior and the vehicle entrance into the network is randomized.

4.2 Experimental Setup based on real data

In this scenario, real data from NGSIM gathered at the American Interstate I-101 [18] are used. This road stretch has a length of 640 m. It consist of five main lanes and it contains an on- and an off-ramp including a weaving lane. Trajectories were gathered over 15 min.

In practice, however, detectors are placed 500 m by 60 s apart on average, for example in the Netherlands. Under these conditions, the the size of the NGSIM data set allows only two detectors and 15 observation instants. Therefore, the setup of both the observation and the prediction model

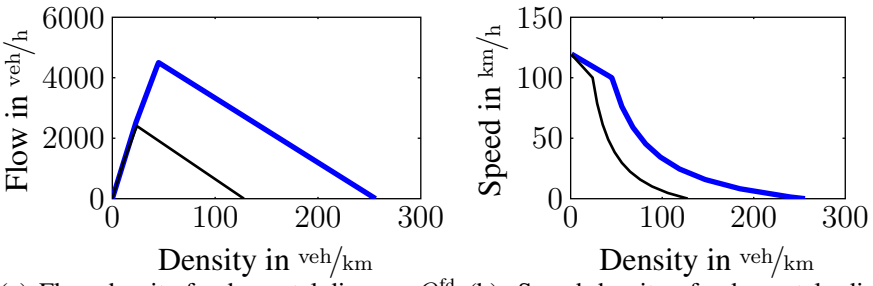

(a) Flow-density fundamental diagram Q^{fd} (b) Speed-density fundamental diagram V^{fd}

FIGURE 4 : **Fundamental diagram used in the filter, estimated in Fosim; bold blue line: two lanes; thin black line: bottleneck of one lane**

are adjusted in order to enable more observations. The virtual detectors are placed at every 100 m and aggregate flows and speeds over 12 s. In the traffic prediction model of the EKF, the cell length is set to 20 m, and the time step length is set to 0.6 s.

The fundamental diagram was calibrated to a capacity of 10000 veh/h and a jam density of 768 veh/km in the 5-lane sections, and 10500 veh/h and 640 veh/km in the 6-lane section. The free speed is set to 100 km/h and the critical speed to 80 km/h. The system state is initialized with an empty road and a variance of $10\,\text{veh}^2/\text{km}^2$ of each cell. The inflow into the prediction model of the EKF is fixed to 5000 veh/h. Since the noise parameters R and Q are difficult to calibrate, several value combinations are analyzed.

In the classic time stepping approach, the Correction step is applied every $\Delta t_{\text{corr}} = \Delta t_{\text{obs}} = 12\,\text{s}$. In the fully-recursive approach, the Correction step is applied in every time step; therefore $\Delta t_{\text{corr}} = \Delta t_{\text{pred}} = 0.6\,\text{s}$.

Ten Monte Carlo simulation have been performed, where the observations were subjected to zero-mean white additive Gaussian noise with a variance of $100\,\text{veh}^2/\text{h}^2$ for flow observations and $5\,\text{km}^2/\text{h}^2$ for speed observations.

4.3 Performance Measurements

The performance of the correction time schemes is evaluated by comparing the estimated states x_k^{e} against the ground truth $\tilde{x}_k$. Two quantities are compared. Firstly, in order to evaluate the spatio-temporal estimation qualities of the filter (like the correct reconstruction of the time and position of congestion), the spatio-temporal density maps are compared. Secondly, in order to compare the total number of vehicles in the network, the densities averaged over time are also evaluated.

Those quantities are compared with the Mean Absolute Error

$$MAE = \frac{1}{I \cdot K} \sum_{i,k} \left| \tilde{x}_{i,k} - x_{i,k}^{\text{e}} \right| \tag{18}$$

and the Root Mean Square Error

$$RMSE = \sqrt{\frac{1}{I \cdot K} \sum_{i,k} \left(\tilde{x}_{i,k} - x_{i,k}^{\text{e}} \right)^2} \,. \tag{19}$$

In addition, the execution times of the filters are compared.

5 RESULTS AND DISCUSSION

This section presents the results of the experiments based on synthetic data in Section 5.1 and based on real data in Section 5.2.

5.1 Results of the experiments based on synthetic data

This section presents the results of the FOSIM experiment set up in Section 4.1.

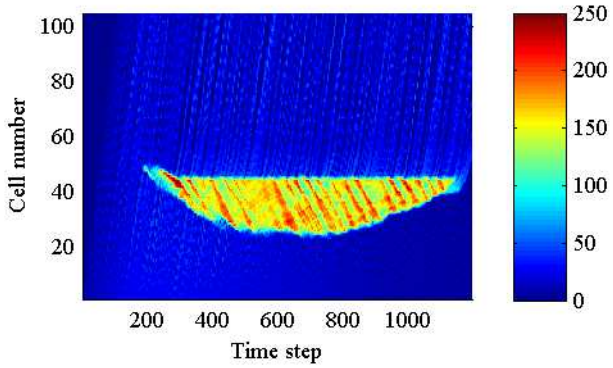

(a) Ground-truth density map

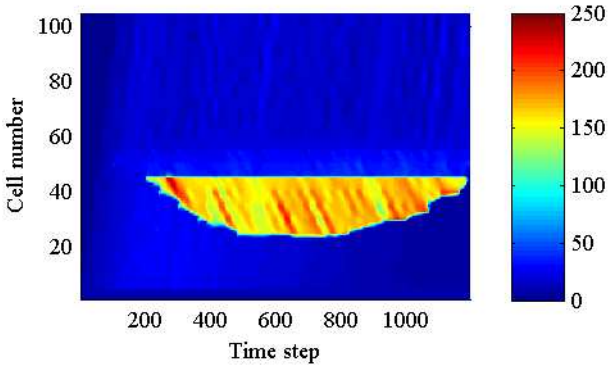

(b) Fully-recursive density map

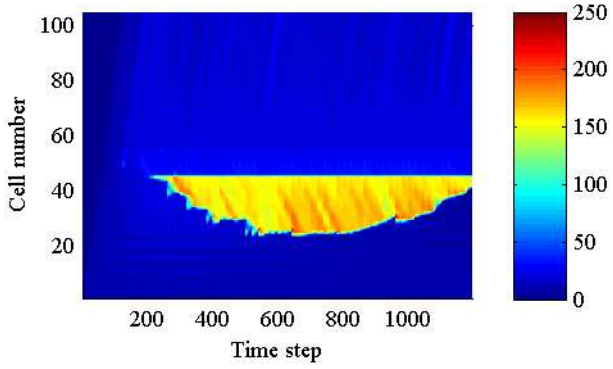

(c) Classic method density map

FIGURE 5 : Density maps (in veh/km) of a simulation run of the FOSIM experiment

Figure 5 contains the density map of the ground truth, the density map of the estimated states x^{e} of the fully-recursive method, and the density map of the classic method (x^{e} if available, otherwise x^{p}) of a simulation run. The ground truth map (Figure 5(a)) clearly shows the congestion at the bottleneck. Furthermore, platoons downstream of the bottleneck are identifiable.

The filter with the fully-recursive correction timing scheme (Figure 5(b)) reconstructed this congestion to a great extend. Position and time of the congestion match with the ground truth. Also, the stop-and-go waves were correctly estimated. This estimate is smoother than in the ground truth, however, because the observations are spread out over one minute, effectively smoothing the density over one minute.

In free flow, the fluctuation in the density caused by the platoon are also reconstructed to an extent. Here, too, these features are not as sharply estimated as in the ground truth, because the observations are aggregated over one minute.

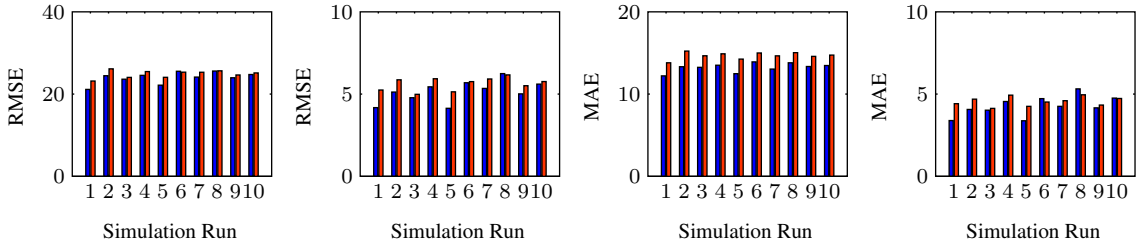

(a) RMSE spatio-temporal density maps (b) RMSE density averaged over time (c) MAE spatio-temporal density maps (d) MAE density averaged over time

FIGURE 6 : **Error measurements of the FOSIM experiments for each of the 10 Monte Carlo simulation runs; blue: fully-recursive scheme, red: classic scheme**

The filter with the classic correction timing scheme (Figure 5(c)) estimates the shape of the congestion roughly. Position and time do not match as accurately as the fully-recursive method. For example, the dissipation of the congestion is estimated too late. Furthermore, the border between free-flow traffic and congested traffic is serrated and does not correctly describe the true transition of the jam.

	fully-recursive ■	**classic** ■
MAE spatio-temporal density in $^{\text{veh}}/_{\text{km}}$	11.0	12.8
MAE density average over time in $^{\text{veh}}/_{\text{km}}$	4.3	4.5
RMSE spatio-temporal density in $^{\text{veh}}/_{\text{km}}$	21.9	22.9
RMSE density average over time in $^{\text{veh}}/_{\text{km}}$	5.2	5.7
Execution time in s	53.4	16.5

TABLE 1 : **Error measurements averaged over 10 Monte Carlo simulation runs**

Figure 6 shows the error measurements applied to each simulation run of both schemes; the values averaged over all simulation runs are listed in Table 1. Comparing the MAE of the spatio-temporal density map, the fully-recursive scheme (11 %) is more precise than the classic scheme (12.8 %). This trend is also vissible in the other error measurements. The fully-recursive scheme therefore outperforms the classic one.

Figure 7 shows a series of density vectors over time of ground truth (green, dashed), the fully-recursive correction timing (blue, solid) and the classic correction timing (red, dotted). The ground truth shows stop-and-go waves between Cells 30 and 45. At Time step 440, a new observation becomes available.

The filter with the fully-recursive scheme closely estimates this stop-and-go wave. Note that the movement of this wave is correctly tracked over time. The filter with the classic correction time scheme, on the other hand, estimates this stop-and-go wave only loosely.

Before an observation becomes available, the density vector of the classic scheme is a smooth line (Figure 7(e)). After the Correction step, the density vector contains fluctuations with local peaks at the observed cells (Figure 7(f)). After a couple of time steps, these local peaks are

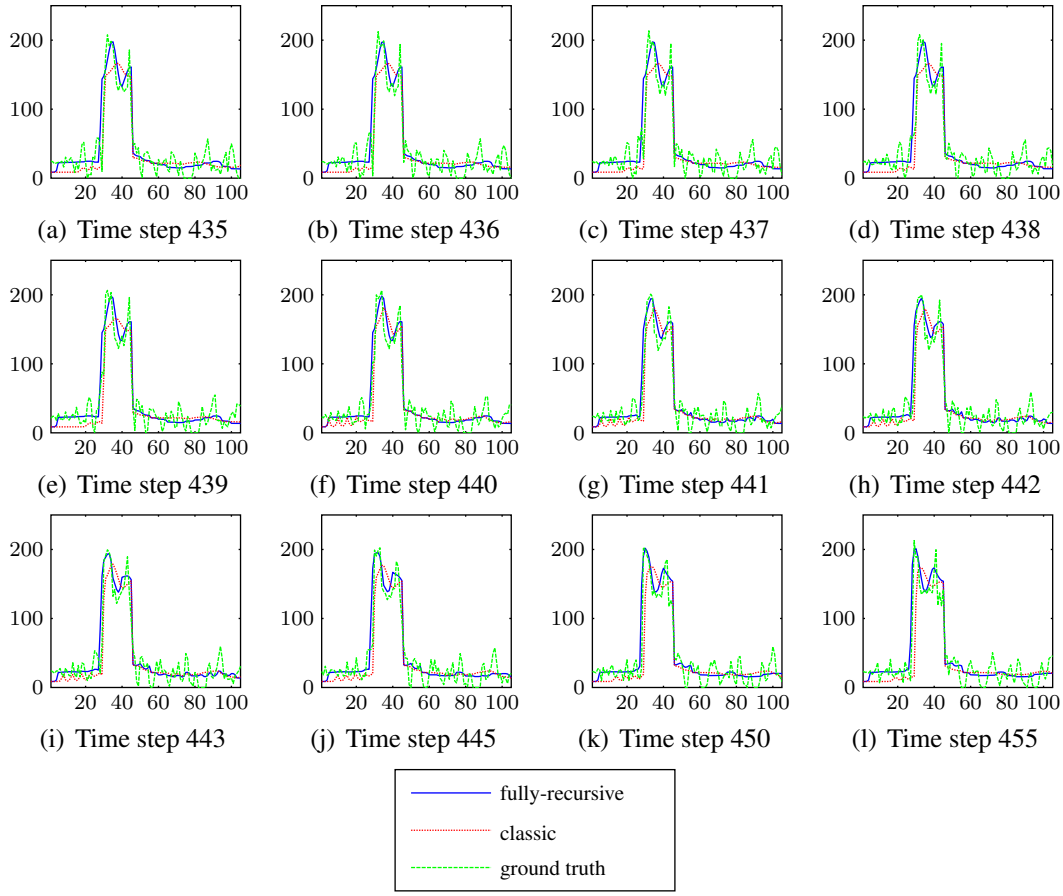

FIGURE 7 : **State vectors of twelve time steps of the fully-recursive correction timing scheme, the classic correction timing scheme and the ground truth; horizontal axis: cell number, vertical axis: density in $^{veh}/_{km}$; at Time step 440 a new observation is available**

smoothed out (Figure 7(g) et seqq.).

The inflow into the network is fixed in the prediction model f, as explained in Section 4.1. In the first four cells, both correction time schemes estimate the densities incorrectly. However, starting with the first observed cell, Cell 5, the fully-recursive correction scheme estimates the density accurately. In contrast, the classic correction scheme miscalculated the density further downstream as well.

Table 1 also presents the execution time of the filters. The filter with the fully-recursive scheme runs within 53 s on average; the filter with the classic scheme runs in a third of this time. The higher execution time of the fully-recursive method is caused, of course, by the higher number of Correction steps that are performed.

5.2 Results of the experiments based on real data

This section presents the results of the simulations based on NGSIM data as described in Section 4.2. Different combinations of error noise matrices R and Q were tested. For the sake of brevity, the results of the combination leading to the highest performance are presented; this is the case for both the system noise matrix Q and the observation noise matrix R of tenfold compared

to the FOSIM setup.

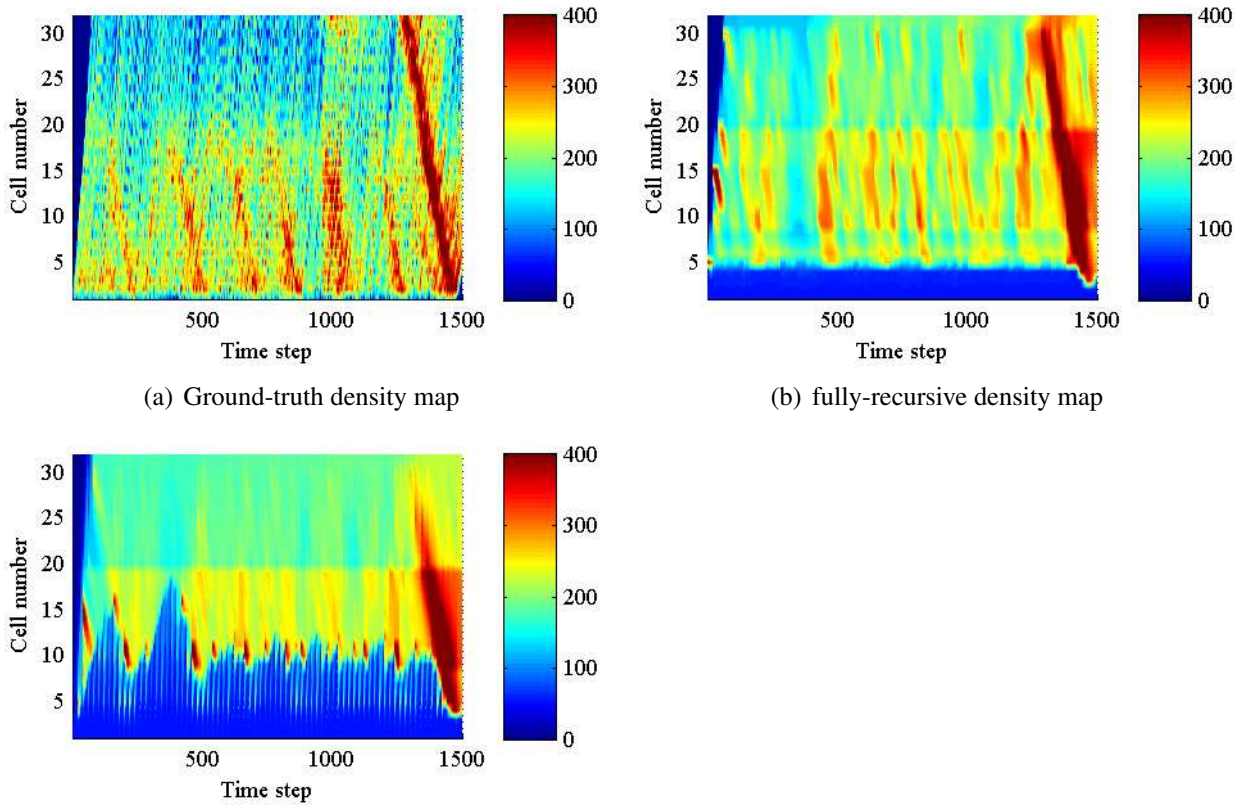

(a) Ground-truth density map

(b) fully-recursive density map

(c) classic method density map

FIGURE 8 : **Density maps (in $^{veh}/_{km}$) of a simulation run of the NGSIM experiment**

In Figure 8, the ground truth and the simulation results the filters with the fully-recursive time stepping scheme and the classic time-stepping scheme are presented. (Note that the road length and simulation time are different than in Figure 5.) In the ground truth (Figure 8(a)), congestion including typical stop-and-go waves can be seen.

The filter with the fully-recursive scheme reconstructs the congestion pattern to some extent (Figure 8(b)). The estimation location and time of the congestion match with the ground truth, starting at the first observed cell. In addition, the large stop-and-go wave near the end of the experiment is reconstructed.

The filter with the classic scheme underestimates the congestion (Figure 8(c)). In particular, even downstream of the first observed cell, the traffic state is erroneously estimated as undersaturated, as the large blue area at the bottom of the plot shows. Also, the large stop-and-go wave near the end of the experiment is reconstructed only partially.

The error measurements are presented in Table 2, averaged over all ten simulation runs. Both MAE and RMSE are large for both schemes. A reason for this might be the unusual setup of narrow detectors both in space and in time. Moreover, due the small data set, the calibration of the parameters is difficult. The traffic is around capacity, which makes it hard to calibrate the

	fully-recursive	**classic**
MAE spatio-temporal density in $^{\mathrm{veh}}/_{\mathrm{km}}$	70.1	85.2
MAE density average over time in $^{\mathrm{veh}}/_{\mathrm{km}}$	20.5	30.1
RMSE spatio-temporal density in $^{\mathrm{veh}}/_{\mathrm{km}}$	94.4	111.6
RMSE density average over time in $^{\mathrm{veh}}/_{\mathrm{km}}$	26.3	36.7
Execution time in s	33.2	17.1

TABLE 2 : **Error measurements averaged over 10 Monte Carlo simulation runs of NGSIM**

fundamental diagram. Furthermore, the noise parameters of the EKF are impossible to determine with such a small data set.

Nevertheless, the filter with the fully-recursive scheme still performs significantly better than the classic scheme, both in terms of the estimated spatio-temporal density and in terms of the estimated number of vehicles in the network.

6 CONCLUSION

In this paper, two correction time schemes of a recursive filter like the Extended Kalman Filter (EKF) were studied. In the classic scheme, the Correction step is applied exactly when a new observation becomes available. In the proposed full-recursive scheme, the Correction step is applied during the whole aggregation time of the observation. In practical traffic applications, where loop detectors continuously observe the flow and the speed, the Correction step is therefore applied in every time step.

Experiments with both synthetic and real data indicate that the fully-recursive method outperforms the classic scheme. Common macroscopic traffic features like stop-and-go waves in congestion or platoons in free flow are estimated with a higher quality. In addition, the total number of vehicles in the network at an instant is better estimated.

This result is intuitive, because every traffic state that contributes to the observation is corrected. In other words, more of the available information is used to estimate the traffic state, which leads to a higher filter quality.

This approach is not restricted to the Extended Kalman Filter, but furthermore applies to recursive filtering in general, for example the Unscented Kalman Filter or Particle Filters.

These results suggest that the quality in online traffic management applications like Dynamic Traffic Management and Advanced Traveler Information Systems is improved by implementing the fully-recursive correction time scheme.

For further research, a more complex network can be studied. Furthermore, this paper used a single-class model; multi-class traffic can be analyzed to apply the results to multi-class models like Fastlane [6], which are in use today.

ACKNOWLEDGMENT

This research work is sponsored under the Research Grant “The MultiModal Port Traffic Centre” by the Port of Rotterdam Authority, Rijkswaterstaat Zuid-Holland and De Verkeersonderneming Rotterdam.

REFERENCES

[1] Treiber, M. and D. Helbing, Reconstructing the Spatio-Temporal Traffic Dynamics from Stationary Detector Data. *Cooper@tive Tr@nsport@tion Dyn@mics*, Vol. 1, No. 3, 2002, pp. 3.1–3.21.

[2] Treiber, M., A. Kesting, and R. E. Wilson, Reconstructing the Traffic State by Fusion of Heterogenous Data. *accepted for publication in Computer-Aided Civil and Infrastructure Engineering*, Vol. preprint `physics/0900.4467`, 2010.

[3] Van Lint, J. and S. P. Hoogendoorn, A Robust and Efficient Method for Fusing Heterogeneous Data from Traffic Sensors on Freeways. *Computer-Aided Civil and Infrastructure Engineering*, Vol. 24, 2009, pp. 1–17.

[4] Schreiter, T., H. van Lint, Y. Yuan, and S. Hoogendoorn, Propagation Wave Speed Estimation of Freeway Traffic with Image Processing Tools. In *in proceeding of the Transportation Research Board, 89th Annual Meeting, Washington, D.C., DVD*, 2010.

[5] Wang, Y., M. Papageorgiou, and A. Messmer, RENAISSANCE–A Unified Macroscopic Model-Based Aapproach to Real-Time Freeway Network Traffic Surveillance. *Transportation Research Part C*, Vol. 14, No. 3, 2006, pp. 190–212.

[6] Van Lint, J., S. Hoogendoorn, and M. Schreuder, Fastlane: New Multiclass First-Order Traffic Flow Model. *Transportation Research Record: Journal of the Transportation Research Board*, Vol. 2088, No. -1, 2008, pp. 177–187.

[7] Ngoduy, D., Applicable Filtering Framework for Online Multiclass Freeway Network Estimation. *Physica A: Statistical Mechanics and its Applications*, Vol. 387, No. 2-3, 2008, pp. 599 – 616.

[8] Xuan, D., H. X. Liu, and G. A. Davis, A Hybrid Extended Kalman Filtering Approach for Traffic Density Estimation along Signalized Arterials Using GPS Data. In *in proceeding of the Transportation Research Board, 89th Annual Meeting, Washington, D.C., DVD*, 2010.

[9] Byon, Y.-J., A. Shalaby, B. Abdulhai, and S. El-Tantawy, Traffic Data Fusion using SCAAT Kalman Filters. In *in proceeding of the Transportation Research Board, 89th Annual Meeting, Washington, D.C., DVD*, 2010.

[10] Work, D., O. Tossavainen, S. Blandin, A. Bayen, T. Iwuchukwu, and K. Tracton, An Ensemble Kalman filtering Approach to Highway Traffic Estimation Using GPS Enabled Mobile Devices. *Proceeding of the 47th IEEE Conference on Decision and Control*, Vol. 47, 2008, pp. 5062–5068.

[11] Lighthill, M. and G. Whitham, On Kinematic Waves. II. A Theory of Traffic Flow on Long Crowded Roads. *Proceedings of the Royal Society of London. Series A, Mathematical and Physical Sciences (1934-1990)*, Vol. 229, No. 1178, 1955, pp. 317–345.

[12] Richards, P., Shock Waves on the Highway. *Operations research*, Vol. 4, No. 1, 1956, pp. 42–51.

[13] van Wageningen-Kessels, F., J. van Lint, S. Hoogendoorn, and C. Vuik, Implicit and Explicit Numerical Methods for Macroscopic Traffic Flow Models. In *TRB 88th Annual Meeting Compendium of Papers DVD*, 2009.

[14] Lebaque, J., The Godunov Scheme and What It Means for First Order Traffic Flow Models, 1996, pp. 647–677.

[15] Sorenson, H., *Kalman filtering: theory and application*. IEEE, 1985.

[16] Kalman, R., A new approach to linear filtering and prediction problems. *Journal of basic Engineering*, Vol. 82, No. 1, 1960, pp. 35–45.

[17] Dijker, T., *FOSIM (Freeway Operations SIMulation)*, 2002.

[18] FHWA, *Next Generation Simulation*. Website: `http://ngsim-community.com/`, 2008.

[19] Edie, L., Discussion of traffic stream measurements and definitions. In *Proceedings*, Organisation for Economic Co-operation and Development, 1965, p. 139.

[20] Courant, R., K. Friedrichs, and H. Lewy, On the partial difference equations of mathematical physics. *IBM Journal*, 1967, pp. 215–234.